Conversion of Elastic Energy Stored in the Legs of a Hexapod Robot into Propulsive Force

Atsushi Kaneko[1]([✉]) [ORCID], Masahiro Shimizu[2] [ORCID], and Takuya Umedachi[1] [ORCID]

[1] Faculty of Textile Science and Technology, Shinshu University,
3-15-1 Tokida, Ueda City, Nagano 386-8567, Japan
{21fs309a,umedachi}@shinshu-u.ac.jp

[2] Department of Systems Innovation, Graduate School of Engineering Science,
Osaka University, 1-2 Machikaneyama-machi, Toyonaka, Osaka 560-0043, Japan
shimizu@sys.es.osaka-u.ac.jp
http://umedachi-lab.com/

Abstract. The conversion of elastic energy due to ground reaction force into propulsive force can help increase the locomotion speed of a legged robot. Many legged robots inspired by animals have been developed, which utilize the elasticity of their legs to increase the efficiency of locomotion. An example is RHex, a hexapod robot that has C-shaped legs. These robots are designed using the spring loaded inverted pendulum (SLIP) model. In contrast, we proposed a new leg design (i.e., D-shaped leg) and an optimization method in which the speed can be increased by kicking the ground strongly in the opposite direction of locomotion due to the elastic force accumulated in the legs. An experiment with a hexapod robot demonstrated that the walking speed could be increased by up to 89% compared to the speed obtained by C-shaped legs. This result can be applied to the design of hands, grippers, and robot bodies to store external force in the flexible body, introduce new functions, and improve performance.

Keywords: Soft robotics · Flexible material · Elastic energy · Legged robot · Optimization

1 Introduction

Many legged robots with flexible and elastic legs, which have been inspired by animals, have been designed to achieve efficient locomotion [1,2]. During the first half of the stance phase of the locomotion of animals, the kinetic and gravitational potential energy are transformed into elastic energy and stored in the legs (especially in their muscles and tendons). In the latter half of the stance phase, this energy is reconverted to the kinetic and gravitational potential energy to accelerate their bodies and generate locomotion efficiently [3]. Many design methods have
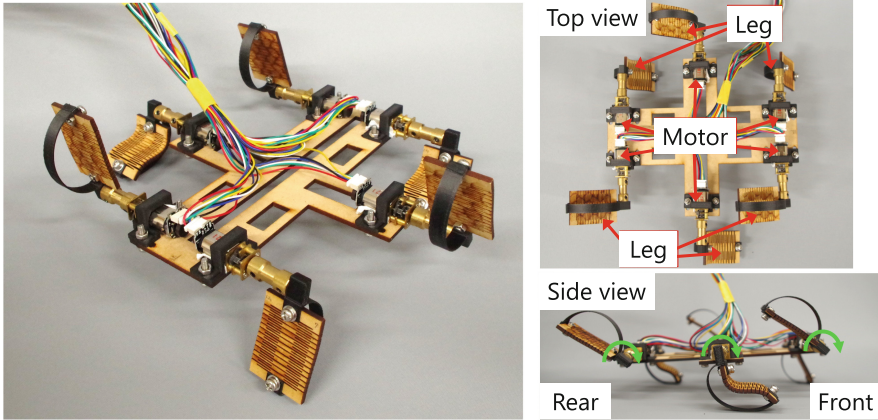
Fig. 1. Prototype (hexapod robot) with the proposed D-shaped legs. The green arrows indicate the direction of the leg rotation when the prototype moves forward. (Color figure online)

been developed and investigated to mimic this efficient mechanism (Sect. 2.1 in [1] and [2]). In these methods, the robot's body is simplified as a mass point and the whole leg as a spring. This simplified model is called the spring loaded inverted pendulum (SLIP) model [4–6] (Fig. 2(d–f)). Here, the spring constant is as stiff as that of an animal's leg of the same mass. RHex [1] and DASH [2] are pioneering examples of the robots designed using the method. It is suggested that these robots can move efficiently by exploiting elastic energy in the legs.

Expeditious advances in rapid prototyping, including 3D printers, have reduced the cost and technical barriers to design and fabricate flexible and complex robotic systems (e.g., robot legs) [7]. Major traditional robotic systems have been composed of rigid mechanical elements. As a result, deformation of the mechanical systems is limited to a few degrees of freedom, such as joints. In contrast, the body parts of living creatures, such as elephant trunks and octopus arms, are composed of flexible materials with complex shapes that deform continuously [8]. By taking advantage of their soft bodies and shapes, living creatures can produce a variety of adaptive behaviors that are difficult for rigid-bodied robotic systems [9]. For example, animals can move over uneven terrain or confined spaces by bending, stretching, or twisting their bodies significantly. It can also grasp objects and the environment with a surface instead of a few contact points. As a result, attempts to employ such flexible and complex mechanical elements in robots have been prevalent in soft robotics [10,11].

This study proposes a novel leg design method to increase the speed of legged robots further using flexible materials. The leg designed by the proposed method is unique because it can convert the elastic energy stored in the leg under normal force into propulsive force. The pioneering SLIP model and the hexapod robot RHex [1] were used as references. However, our proposed method differs from the previous methods because our proposed leg *deforms to produce a greater*

propulsive force. We compare the walking performance of the proposed method with the existing method with a prototype. The experimental results show that the proposed method can accelerate locomotion by up to 89%. Furthermore, it is considered to have the potential to be applied to various soft robot parts such as hand, gripper, and body design and is not limited to only legs. The proposed method converts the externally obtained force once into an elastic force and uses it for the desired function.

2   Related Works

A typical model of locomotion in animals is the SLIP model [4–6] (see Fig. 2(d–f)). Studies on various animals [6] have shown that the stiffness of the leg spring tends to be proportional to the 0.67 power of the body mass. Animals can use the elasticity of the leg for efficient locomotion.

Inspired by this biological finding, some studies have suggested that appropriately designing a robot's leg spring stiffness can help improve its performance in terms of locomotion efficiency and suppression of disturbances from the ground during locomotion [12,13]. The robots in [1,2,14] are excellent examples of adjusting the stiffness of the leg spring to improve locomotion performance.

Existing pioneering research that attempts to improve mobility performance by utilizing soft parts in robots and excellent jumping robots that use elastic energy are described. Mahkam et al. [15] showed that when the robot uses compliant backbones and legs, the locomotion speed is improved compared to that when rigid ones are used. Spröwitz et al. [16] reported that attaching compliant elements to the robot's toes increased its maximum speed. Brown et al. [17] developed the Bow Leg that can move with low power consumption. The behavior during locomotion is different from our robot because this leg is used for hopping, and the driving mechanism is different; however, the shape of the Bow Leg is similar to that of our leg proposed in this study. In [18], Mochiyama et al. described the mechanism of generating instantaneous force by buckling for jumping. In contrast, in this study, the propulsive force is increased by utilizing the energy stored in the legs and simply releasing it.

3   Proposed Method

The concept of our proposed model is shown in Fig. 2(a–c). This study proposes to add a torsion spring in the leg model (SLIP model in Fig. 2(d–f)) to increase the propulsive force by designing these stiffnesses appropriately. In this paper, the newly-added torsion spring is called "leg torsion spring", and the spring inherited from the SLIP model is called "leg linear spring".

3.1   D-Shaped Leg

We propose a D-shaped leg that converts elastic energy stored by the normal force from the ground into propulsive force. If a robot's legs can kick the ground
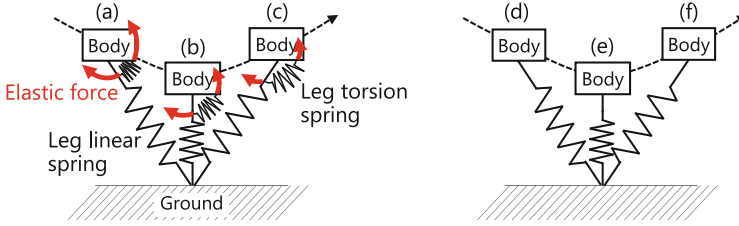
Fig. 2. Concept of the proposed model and the different interaction with the ground between the proposed and existing SLIP models during the locomotion. This figure shows the two models moving to the right. (a–c) show a new model with a torsion spring added to the SLIP model. In (a), the leg touches the ground, the torsion spring is compressed, and elastic energy is stored in the torsion spring. In (b, c), the elastic energy stored in the torsion spring is released, and the body is pushed forward. The linear spring is drawn assuming that it deforms similarly as in the SLIP model. (d–f) show the SLIP model [4–6].

strongly in the opposite direction of locomotion due to elastic force, it can achieve a large propulsive force that increases its speed. For this, the legs must store a large amount of elastic energy just before they kick the ground. The direction of the elastic force generated by the legs is also essential. If the legs are deformed in such a way that the toes project forward (as in Fig. 3(a–c)) just before the legs kick the ground, the elastic force acts to push the body forward. The greater the protrusion, the more effectively the legs push the body forward. The D-shaped leg is based on the C-shaped leg in the previous study (Sect. 3.4 of [1]) and combines a C-shaped component with an I-shape beam (see Fig. 3(d, e)). Each D-shaped leg has a rubber pad on the toe to increase friction with the ground.

The D-shaped leg is designed by a combination of physical simulation and optimization with the following two policies:

  i) To maximize the elastic energy stored in the leg just before kicking the ground
 ii) To adjust the stiffness of the leg linear spring based on the mass of the robot as in the previous study (Sect. 2.1 of [1])

Like the C-shaped leg, the D-shaped leg rolls as the robot locomotes, so the point of contact with the ground changes from the hip side to the toe (see Fig. 3(a–c)). In this study, a static simulation is performed for the state just before the leg kicks the ground. As described below (see Sect. 3.3), each D-shaped leg is composed largely of a material with a relatively low damping coefficient; therefore, static simulation could be used. Then, in Sect. 4, the performances of the D-shaped legs and the C-shaped legs fabricated based on the design method of the previous study (Sect. 2.1 of [1]) were compared. For a fair comparison, the stiffnesses of the leg linear spring of the two legs should be the same; therefore, ii) was included in the design policies.

For physical simulation, entire D-shaped leg is modeled as springs and torsion springs (see Fig. 3(f)). This is a two-dimensional simplified version of a D-shaped

leg, focusing on the deformation in the case viewed from the side. As shown in Fig. 3(f), the D-shaped leg is divided into a C-shaped and an I-shaped part. The stiffnesses of the torsion springs in each C-shaped and I-shaped section are used as variables in the optimization. The torsion springs were varied uniformly in each of the two parts. The range of possible values for the torsion spring's stiffness variables and the adopted linear spring's stiffness are shown in Table 1. After making samples of each part and ascertaining the range of stiffnesses that could be fabricated, the range of variables was determined. The stiffnesses of the linear springs are set to the values obtained when the legs are fabricated by the manufacturing method described below.
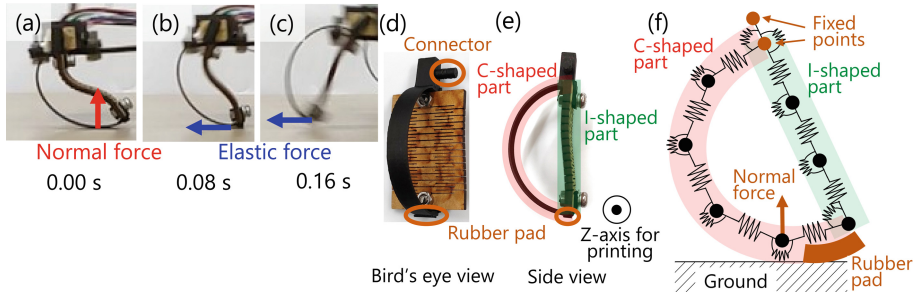

Fig. 3. (a–c) show the deformation of the D-shaped leg during locomotion. At (a), the D-shaped leg touches the ground, and the normal force from the ground deforms the leg forward. In (b, c), the elastic force of the leg acts as a propulsive force. (d, e) show the fabricated D-shaped leg. We attached a 2 mm long rubber pad to toe of the D-shaped leg. We connect the leg to the motor with the connector part on the top. (f) shows the simulation model of the D-shaped leg. The leg is fixed at the orange point at the top, and 0.7 N (i.e., the weight of the robot divided by the number of supporting legs (3)) is applied to the edge of the C-shaped part of the rubber pad as the normal force.

We used the above simulation model to perform a static simulation that reproduces the state just before the leg kicks the ground. In the prototype, the leg is connected to the body at the upper part (i.e., connector in Fig. 3(d)). Thus, in the simulation, the leg is fixed at the same point as shown in Fig. 3(f). The forces actually applied to the leg are the normal force from the ground, the friction force, and the force from the connection with the body. The normal force is applied in the direction and at the force point as shown in Fig. 3(f), taking into account the inclination of the leg at this moment. The magnitude of the force is the weight of the robot per leg (i.e., the weight of the robot divided by the number of supporting legs (3), 0.7 N). The friction force from the ground is not considered in this optimization design because the objective is to design the D-shaped leg so that the normal force generated by the robot's weight can be converted into a force to kick the ground.

3.2 Optimization of D-Shaped Leg

To perform the above simulation and optimization, we used Rhinoceros 6, a 3D CAD system, and its plug-in, Grasshopper, which includes a physical simulator.

Table 1. Simulation settings.

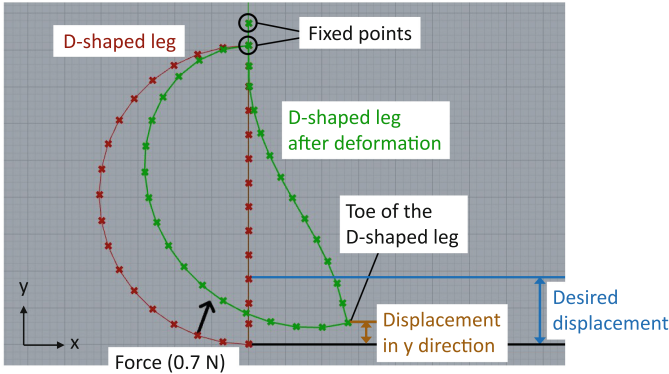| Parameter	Value
Range of torsion spring's stiffness in the C-shaped part	20–50000 N · mm/rad
Range of torsion spring's stiffness in the I-shaped part	5–50000 N · mm/rad
Stiffness of the C-shaped part's linear springs	530 N/mm
Stiffness of the I-shaped part's linear springs	66000 N/mm

Fig. 4. Deformation of the D-shaped leg (simulated in Rhinoceros) and explanation of the optimization design. As shown in Fig. 3(f), a model of the D-shaped leg has been created, but no spring is shown in this figure. The leg was fixed at the top two points and the force of the thick black arrow was applied. The plots in red and green show the D-shaped leg before and after deformation, respectively. (Color figure online)

Figure 4 shows the deformation of the simulation model of the D-shaped leg in Rhinoceros during the static simulation as described above.

We set up two objective functions corresponding to the design policies i) and ii) and performed a multi-objective optimization. The objective function for i) was set to maximize the elastic energy stored in the leg after deformation, whereas the objective function for ii) was set to minimize the difference between the y-direction displacement of the toe of the D-shaped leg (see Fig. 4) and the desired displacement as described below. The elastic energy stored in the leg after deformation is obtained by the following equation.

$$E = \sum \frac{1}{2} k_\theta \Delta\theta^2 + \sum \frac{1}{2} k_l \Delta l^2 \tag{1}$$

E is the sum of the elastic energy stored in the leg, k_θ is the stiffness of the torsion spring, $\Delta\theta$ is the angular displacement of each torsion spring, k_l is the stiffness of the linear spring, and Δl is the change in the length of each linear spring. The objective function of ii) is

$$f(y) = |y - y_{target}| \tag{2}$$

Table 2. Optimization parameters.

Parameter	Value
Population size	100
Mutation rate	0.9
Mutation probability	0.2
Crossover rate	0.8
Max generation	25
Elitism	0.7

Table 3. Optimization results.

Parameter	Value
Stiffnesses of the C-shaped part's torsion springs	$476.50 \text{ N} \cdot \text{mm/rad}$
Flexural rigidity of the C-shaped part	$529 \text{ N} \cdot \text{mm}^2$
Stiffnesses of the I-shaped part's torsion springs	$49.81 \text{ N} \cdot \text{mm/rad}$
Flexural rigidity of the I-shaped part	$38 \text{ N} \cdot \text{mm}^2$

where y is the displacement of the toe in the y-direction after deformation, and y_{target} is the desired displacement required to achieve the appropriate stiffness of the leg linear spring (These can be displayed on the Rhinoceros screen as shown in Fig. 4). The appropriate stiffness of the leg linear spring is obtained from Fig. 3C of [6], and the mass of the prototype (0.21 kg). The appropriate stiffness of the leg linear spring for this mass is 230 N/m. From the number of supporting legs (3) and the normal force applied to the leg during locomotion (0.70 N), the required leg displacement y_{target} can be obtained by the following equation.

$$y_{target} = \frac{0.70}{\frac{230}{3}} = 0.0091 \tag{3}$$

From this equation, y_{target} is 9.1 mm. The optimization was performed using a genetic algorithm (named Octopus[1] as a Grasshopper plug-in). We chose genetic algorithms as they are versatile. Octopus performed a multiobjective evolutionary algorithm called HypE [19]. The parameters related to the optimization are shown in Table 2. From the optimization, the stiffnesses of the torsion springs of the C-shaped and I-shaped parts were obtained. The bending stiffness values of each part were obtained from these stiffnesses using the Rhinoceros simulation. The results are shown in Table 3.

3.3 Fabrication of the Leg

The C-shaped and I-shaped parts were fabricated to achieve the bending stiffness obtained from the simulation, respectively. The C-shaped part was fabricated by

---

[1] Octopus, a Grasshopper plug-in: https://www.food4rhino.com/en/app/octopus.

Table 4. Parameters of the prototype.

Body mass			210 g
Body		Length	165 mm
		Width	138 mm
Length of both the D-shaped leg and C-shaped leg			50 mm
D-shaped leg	I-shaped part (2D repetitive slit pattern)	Length	41 mm
		Width	28 mm
		Thickness	2.5 mm
	C-shaped part	Width	7 mm
		Thickness	0.7 mm
C-shaped leg		Width	15 mm
		Thickness	0.7 mm

a 3D printer (MarkTwo, Markforged) using a nylon-based filament (Onyx) at 100% fill rate. The z-axis for 3D printing of the C-shaped part is displayed in Fig. 3(e). The I-shaped part was comprised of a 2D repetitive slit pattern cut [20] from a 2.5 mm thick MDF (fiberboard made of wood) by a laser cutting machine (VLS6.60, Universal Laser Systems). We used this method because the slit can significantly reduce the bending stiffness, and the bending stiffness can be varied by changing the number of slits [20].

4   Experiment

4.1   Fabrication of the Prototype

We fabricated the prototype to compare the locomotion performances of the D-shaped legs proposed in this study and the C-shaped legs fabricated by the design method proposed in Sect. 2.1 of [1]. The comparison was made by changing the legs attached to the prototype. Six DC motors (model number 3043, gear ratio 210:1, Pololu) were fixed to the body as shown in Fig. 1. Each leg is rotated by one motor to realize locomotion with six legs, similar to RHex [1]. The rotation of each motor that drives the legs was sensed by rotary encoders (model number 4760, Pololu) and controlled by microcontrollers (LPC1768, NXP). Power was supplied to the motors via motor drivers (TB6612FNG, Toshiba) with a 12.0 V input. The body was composed of a 2.5 mm thick MDF, which is relatively light and rigid. The mass and dimensions of the prototype are specified in Table 4.

The C-shaped leg is designed similarly as in Sect. 2.1 of [1], i.e., the stiffness of the leg linear spring should be appropriate for the mass of the robot. The appropriate stiffness for the prototype is 230 N/m from Sect. 3.2. From Castigliano's theorem, the displacement of the tip of a curved bar when a force is applied to it can be determined (Sect. 80 of [21] provides more details). Therefore, when we consider the C-shaped leg as a curved bar, the stiffness of the leg linear spring
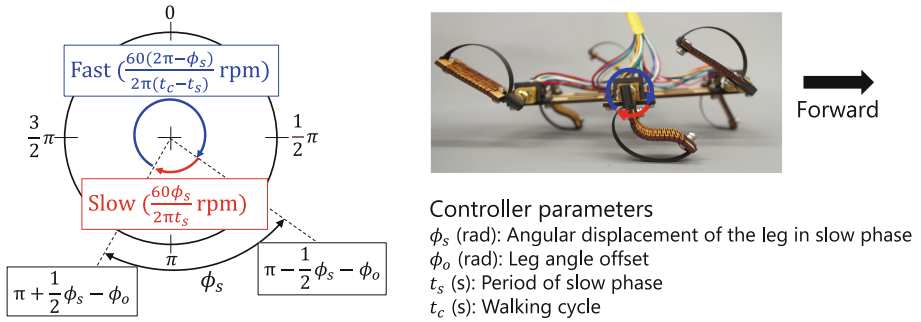
Fig. 5. Rotation of the right leg of the robot when the robot moves forward toward the right side. The angle of the transition from fast phase to slow phase, the angle of the transition from slow phase to fast phase, and the rotation speed of the motor in each phase are written. This control is based on [22,23].

can be obtained based on the relationship between the force applied to the toe and the displacement of the toe. In this way, we adjusted the dimensions of the C-shaped leg appropriately and fabricated the leg with Onyx using the above mentioned 3D printer. We attached a rubber pad to each toe.

4.2   Control of the Prototype

The controller parameters of previous studies [22,23] are used as a reference for control of the prototype (see Fig. 5). This is because the prototype, similar to RHex, moves by repeatedly rotating its legs. From the previous study [22], it can be determined that there are four essential controller parameters when using C-shaped legs and moving forward with a tripod gait, as shown in Fig. 5.

When starting locomotion, the desired angle of each leg is first calculated from the four parameters as shown in Fig. 5. Then, the PD control of the motor is performed so that the encoder value is close to the calculated value. The walking cycle is t_c [s]. As shown in Fig. 5, there are two phases in the cycle, the "fast phase" and "slow phase". In the fast phase, the motor rotates the leg by $2\pi - \phi_s$ [rad] during $t_c - t_s$ [s]. In the slow phase, the motor rotates the leg by ϕ_s [rad] during t_s [s]. When ϕ_o is 0, the range from $\pi - \frac{1}{2}\phi_s$ to $\pi + \frac{1}{2}\phi_s$ corresponds to the slow phase. Otherwise, the angle of the slow phase is shifted by ϕ_o as shown in Fig. 5. This process is repeated during the locomotion.

The six legs are divided into two sets, each synchronized separately. One set is right front, right rear, and left middle, and the other is left front, left rear, and right middle. The former three legs are 180° out of phase with the latter three legs. The details are described in previous studies [22,23].

4.3   Experimental Results

We measured and compared the locomotion speed of the robot with the D-shaped legs proposed in Sect. 3.1 and the C-shaped legs described in Sect. 4.1.

Table 5. Experimental results of locomotion speeds obtained with the D-shaped legs and C-shaped legs when $t_s = 0.38$ and $t_c = 0.76$. Crosses indicate that the body often touched the ground and the experiment was not performed. (a) The ratio (in percent) of the speed with the D-shaped leg to the speed with the C-shaped leg. A ratio of 100% indicates that the two speeds are the same. The deeper the red color, the faster the speed with the D-shaped leg compared to the speed with the C-shaped leg. (b, c) Locomotion speed of the prototype with the D-shaped and C-shaped legs, respectively. The units are meters per second.

(a) Comparison of the D-shaped legs and C-shaped legs [%]

ϕ_o \ ϕ_s	0.4	0.8	1.2	1.6	
0.8	×	×	×	×	200
0.4	189	163	132	×	150
0.0	120	148	144	122	100
-0.4	136	125	122	×	50
-0.8	×	×	×	×	0

(b) Locomotion speed with the D-shaped legs [m/s]

ϕ_o \ ϕ_s	0.4	0.8	1.2	1.6
0.8	×	×	×	×
0.4	0.18	0.19	0.20	×
0.0	0.073	0.14	0.21	0.25
-0.4	0.16	0.21	0.24	×
-0.8	×	×	×	×

(c) Locomotion speed with the C-shaped legs [m/s]

ϕ_o \ ϕ_s	0.4	0.8	1.2	1.6	
0.8	×	×	×	×	0.25
0.4	0.10	0.11	0.15	×	0.20
0.0	0.061	0.093	0.15	0.20	0.15
-0.4	0.12	0.17	0.20	×	0.10
-0.8	×	×	×	×	0.05
					0.00

The prototype moved for five periods, the distance traveled was measured, and the speed was calculated. Since the robot has a relatively small mass, the average speed was obtained by dividing the distance traveled by the elapsed time without considering the time for acceleration or deceleration. We experimented with different motor controller parameters ϕ_s and ϕ_o as described in Sect. 4.1. We varied these parameters to the extent that the body did not touch the ground and the body was not dragged. The remaining parameters, t_s and t_c, were set as 0.38 s and 0.76 s, respectively. First, we repeated the locomotion three times with each parameter setting and obtained the average value. The velocities of the prototypes with the D-shaped legs and C-shaped legs are shown in Table 5.

The results (Table 5) show that the locomotion speed is up to 1.89 times greater when using the D-shaped legs than when using the C-shaped legs. The
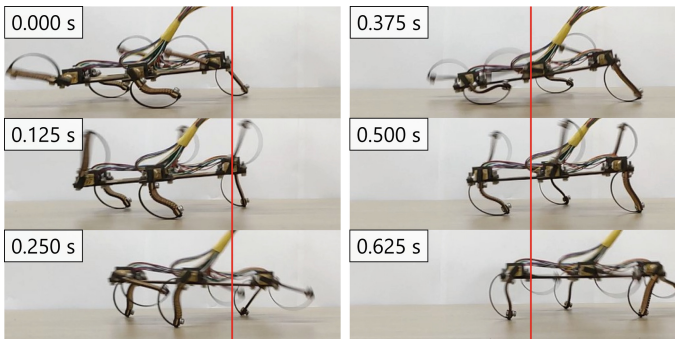

Fig. 6. Snapshots of the prototype with D-shaped legs during locomotion ($\phi_s = 1.6$, $\phi_o = 0.0$). The snapshots show that the legs are deformed as in the simulation, and the legs kick the ground. The red line denotes the position of the head of the prototype at 0.000 s (Color figure online).

difference depends on the controller parameters ϕ_s and ϕ_o. As shown in Fig. 6, the D-shaped legs are deformed in such a way that the toes project forward during the stance phase. The increase in speed is thought to be due to the utilization of the elastic force generated by the deformation to kick the ground.

5   Conclusion

We demonstrated a method of designing legs that can increase locomotion speed by utilizing the elastic force of the legs to produce a propulsive force. In this design method, a new leg model with a "leg torsion spring" added to the SLIP model is considered, and the propulsive force is increased according to the design of an appropriate stiffness of the entire leg. In this study, a D-shaped leg is proposed to effectively convert elastic force into propulsive force when it is subjected to normal force. Physical simulations and optimization of the D-shaped leg were carried out to obtain a strong propulsive force. C-shaped and I-shaped parts were fabricated to match the bending stiffness obtained from the simulation. D-shaped legs were fabricated by combining these two parts. We compared the locomotion speed of the prototype with the D-shaped legs and that with the C-shaped legs fabricated by a design method of a previous study [1]. The experimental results show that the locomotion speed of the D-shaped legs is faster than that of the C-shaped legs, and the locomotion speed increases up to 1.89 times. In the case of the D-shaped leg, it was confirmed that the toe projected forward in the stance phase, as intended in the design phase (as in Fig. 3(a–c)).

In a further study, we will perform simulations and optimizations of the D-shaped leg, including the stiffnesses of the linear springs, as variables. In this study, we added a restriction so that the stiffnesses of the torsion springs could be uniform. We believe that by removing this restriction, we can further increase the elastic energy stored in the leg. We will also conduct an experiment to investigate the locomotion speed by rotating the legs at a higher speed, and we will compare the moving speed when t_s and t_c are changed.

References

1. Moore, E.Z.: Leg design and stair climbing control for the RHex robotic hexapod. Masters thesis (2002)
2. Birkmeyer, P., Peterson, K., Fearing, R.S.: DASH: a dynamic 16g hexapedal robot. In: 2009 IEEE/RSJ International Conference on Intelligent Robots and Systems, pp. 2683–2689 (2009)
3. Dickinson, M.H., Farley, C.T., Full, R.J., Koehl, M.A.R., Kram, R., Lehman, S.: How animals move: an integrative view. Science **288**, 100–106 (2000)

4. Blickhan, R.: The spring-mass model for running and hopping. J. Biomech. **22**, 1217–1227 (1989)
5. Hubicki, C., et al.: ATRIAS: design and validation of a tether-free 3D-capable spring-mass bipedal robot. Int. J. Robot. Res. **35**, 1497–1521 (2016)
6. Farley, C.T., Glasheen, J., McMahon, T.A.: Running springs: speed and animal size. J. Exp. Biol. **185**, 71–86 (1993)
7. Rus, D., Tolley, M.T.: Design, fabrication and control of soft robots. Nature **521**, 467–475 (2015)
8. Trivedi, D., Rahn, C.D., Kier, W.M., Walker, I.D.: Soft robotics: biological inspiration, state of the art, and future research. Appl. Bionics Biomech. **5**, 99–117 (2008)
9. Kim, S., Laschi, C., Trimmer, B.: Soft robotics: a bioinspired evolution in robotics. Trends Biotechnol. **31**, 287–294 (2013)
10. Pfeifer, R., Lungarella, M., Iida, F.: The challenges ahead for bio-inspired "soft" robotics. Commun. ACM **55**, 76–87 (2012)
11. Laschi, C., Cianchetti, M., Mazzolai, B., Margheri, L., Follador, M., Dario, P.: Soft robot arm inspired by the octopus. Adv. Robot. **26**, 709–727 (2012)
12. Calisti, M., Picardi, G., Laschi, C.: Fundamentals of soft robot locomotion. J. Roy. Soc. Interface **14**, 1–2 (2017)
13. Galloway, K.C., Clark, J.E., Koditschek, D.E.: Variable stiffness legs for robust, efficient, and stable dynamic running. J. Mech. Robot. **5**, 011009 (2013)
14. Galloway, K.C., Clark, J.E., Yim, M., Koditschek, D.E.: Experimental investigations into the role of passive variable compliant legs for dynamic robotic locomotion. In: 2011 IEEE International Conference on Robotics and Automation, pp. 1243–1249 (2011)
15. Mahkam, N., Yilmaz, T.B., Ozcan, O.: Smooth and inclined surface locomotion and obstacle scaling of a C-legged miniature modular robot. In: 2021 IEEE 4th International Conference on Soft Robotics (RoboSoft), pp. 9–14 (2021)
16. Spröwitz, A., Tuleu, A., Vespignani, M., Ajallooeian, M., Badri, E., Ijspeert, A.J.: Towards dynamic trot gait locomotion: design, control, and experiments with Cheetah-cub, a compliant quadruped robot. Int. J. Robot. Res. **32**, 932–950 (2013)
17. Brown, B., Zeglin, G.: The bow leg hopping robot. In: Proceedings of the 1998 IEEE International Conference on Robotics and Automation, pp. 781–786 (1998)
18. Tsuda, T., Mochiyama, H., Fujimoto, H.: Quick stair-climbing using snapthrough buckling of closed elastica. In: 2012 International Symposium on Micro-NanoMechatronics and Human Science (MHS), pp. 368–373 (2012)
19. Bader, J., Zitzler, E.: HypE: an algorithm for fast hypervolume-based manyobjective optimization. Evol. Comput. **19**, 45–76 (2011)
20. Ohshima, T., Tachi, T., Yamaguchi, Y.: Analysis and design of elastic materials formed using 2D repetitive slit pattern. In: Proceedings of the International Association for Shell and Spatial Structures Symposium, IASS 2015, pp. 526418:1–526418:12 (2015)
21. Timoshenko, S.: Strength of Materials, Vol. I : Elementary Theory and Problems (English Edition). CBS Publishers & Distributors Pvt Ltd. (2004)
22. Saranli, U., Buehler, M., Koditschek, D.E.: RHex: a simple and highly mobile hexapod robot. Int. J. Robot. Res. **20**, 616–631 (2001)
23. Weingarten, J.D., Lopes, G.A.D., Buehler, M., Groff, R.E., Koditschek, D.E.: Automated gait adaptation for legged robots. In: Proceedings - IEEE International Conference on Robotics and Automation, pp. 2153–2158 (2004)